24. B. J. Geldzahler *et al.*, *Astrophys. J.* **273**, L65 (1983).
25. M. F. Cawley *et al.*, *ibid.* **296**, 185 (1985).
26. D. R. Parsignault *et al.*, *Nature (London) Phys. Sci.* **239**, 123 (1972).
27. A. A. Watson, in *Proceedings of the 19th International Cosmic Ray Conference* (NASA Conference Publication 2376, Springfield, VA, 1985), vol. 9, p. 111.
28. Yu. I. Neshpor *et al.*, *Astrophys. Space Sci.* **61**, 349 (1979).
29. A. M. Hillas, in *Very High Energy Gamma-Ray Astronomy*, K. E. Turver, Ed. (Reidel, Dordrecht, 1987), p. 71.
30. R. J. Gould, *Astrophys. J.* **271**, L23 (1983); M. F. Cawley and T. C. Weekes, *Astron. Astrophys.* **133**, 80 (1984); R. J. Protheroe, in *Proceedings of the 19th International Cosmic Ray Conference* (NASA Conference Publication 2376, Springfield, VA, 1985), vol. 1, p. 297.
31. J. M. Dickey, *Astrophys J.* **273**, L71 (1983).
32. A. M. Hillas, *Nature (London)* **312**, 50 (1984); V. J. Stenger, *Astrophys. J.* **284**, 810 (1984).
33. G. Ballistoni *et al.*, *Phys. Lett. B* **155**, 465 (1985); M. L. Marshak *et al.*, *Phys. Rev. Lett.* **55**, 1965 (1985).
34. P. Bareyre *et al.* in *Proceedings of the 19th International Cosmic Ray Conference* (NASA Conference Publication 2376, Springfield, VA, 1985), vol. 9, p. 465; Y. Oyama *et al.*, *Phys. Rev. Lett.* **56**, 991 (1986). G. Chardin and G. Gerbier, *Proceedings of the 20th International Cosmic Ray Conference* (Nauka, Moscow, 1987), vol. 1, p. 236.
35. W. T. Vestrand and D. Eichler, *Astrophys. J.* **261**, 251 (1982).
36. J. M. Cohen and E. Mustafa, *ibid.* **319**, 930 (1987).
37. D. Eichler and W. T. Vestrand, *Nature (London)* **307**, 613 (1984).
38. ———, *ibid.* **318**, 345 (1985).
39. D. Kazanas and D. C. Ellison, *ibid.* **319**, 380 (1986).
40. G. Chanmugam and K. Brecher, *ibid.* **313**, 767 (1985).
41. This work is supported by the U.S. Department of Energy.

Wind-Driven Ocean Currents and Ekman Transport

JAMES F. PRICE, ROBERT A. WELLER, REBECCA R. SCHUDLICH

Oceanographers have long sought to verify the theoretical Ekman transport relation, which predicts that a steady wind stress acting together with the Coriolis force will produce a transport of water to the right of the wind. In situ measurements of wind and ocean currents provide a detailed view of this phenomenon. By separating the wind-driven current from the measured total current and by averaging over a long record, it is found that the observed transport is consistent with theoretical Ekman transport to within about 10 percent. In this case the wind-driven transport is strongly surface trapped, with 95 percent occurring in the upper 25 meters as a result of fair summer weather.

THE STARTING POINT FOR MODERN THEORIES OF WIND-driven ocean circulation can be traced to Ekman's (*1*) theoretical study on the direct effect of wind stress on ocean currents. Ekman's theory was the first to acknowledge that vertical mixing in the upper ocean is caused by turbulence. He proposed that turbulent mixing could be modeled as a diffusion process, exactly analogous to molecular diffusion, but with an effective (kinematic) viscosity, A, many orders of magnitude larger than molecular viscosity. The value of A appropriate to the upper ocean was left to be determined from observations. By assuming that the momentum balance of a steady wind-driven current was between the turbulent stress caused by the wind and the Coriolis force caused by the earth's rotation, Ekman derived the archetypal solution for the vertical structure of a wind-driven current

$$[u, v] = \mathbf{V}_0 \exp(-z/D)\ [\cos(\pi/4 - z/D), \sin(\pi/4 - z/D)] \qquad (1)$$

J. F. Price and R. A. Weller are associate scientists in the Physical Oceanography Department of the Woods Hole Oceanographic Institution, Woods Hole, MA 02543. R. R. Schudlich is a Ph.D. candidate in the Joint Program in Oceanography and Oceanographic Engineering of the Woods Hole Oceanographic Institution and the Massachusetts Institute of Technology, Woods Hole, MA 02543.

where $[u, v]$ are, respectively, east and north current components; wind stress is assumed northward $[0, \tau]$; $\mathbf{V}_0 = \tau/\rho(Af)^{1/2}$ is the surface amplitude; $D = (2A/f)^{1/2}$ is the e-folding scale depth; z is depth taken positive downward; and ρ is the density of seawater that can be assumed constant. The Coriolis parameter f is equal to twice the vertical component of the earth's rotation vector, and in the Northern Hemisphere (assumed throughout), $f > 0$.

There are two noteworthy results from Eq. 1. The first is that the current profile from Ekman's theory has a spiral structure, called an Ekman spiral, in which current amplitude decays by one e-folding over a depth D as the current vector rotates to the right through 1 radian. Observations of ocean currents have often been fitted to this form in order to infer A, as Ekman suggested. Typical values are $D = 30$ m and $A = 500 \times 10^{-4}$ m^2 sec^{-1}. However, the range of inferred A covers more than an order of magnitude (*2, 3*) so that neither A nor D can be regarded as well known. The detailed specific structure of the spiral depends on A being constant in depth and time, which now seems unlikely to hold in the upper ocean (*2*). So-called turbulent Ekman theories have been developed to model the possible depth and time dependence of A (*4*). These theories yield somewhat different spiral structures, but there is no consensus on, for example, the sense of the depth dependence of A. The structure of the mean wind-driven current thus remains an open theoretical question.

A second and fundamental result from Eq. 1 is that the vertically integrated current, or volume transport per unit width, is given by the Ekman transport relation

$$\int_0^{z_r} [u, v]dz = [\tau/\rho f, 0] \qquad (2)$$

where z_r is the depth below which the wind-driven current vanishes. If the Ekman spiral solution were applicable, then $z_r = 3D$ would be an excellent approximation. But just as D is not known beforehand with confidence, neither is z_r. However, the magnitude and direction of the transport follow directly from the presumed momentum balance between wind stress and the Coriolis force and are independent of A or any other aspect of vertical mixing (*5*). Equation 2 shows that in the Northern Hemisphere the wind-driven transport is expected to be 90° to the right of the wind stress vector. This has profound consequences for the general circulation and climate of the ocean. For example, the persistent easterly trade winds in the lower subtropics are expected to drive a northward Ekman transport of warm water toward the pole. Westerly winds at mid-latitudes are expected to drive a southward Ekman transport so that a convergence should occur in the subtropical oceans. The result should be a thick warm water layer above the main thermocline and, through conservation of potential vorticity, a clockwise general circulation in a subtropical gyre. These are major, observed features of the subtropical oceans and are strong but indirect evidence that some process like Ekman transport must play a crucial role in shaping the ocean's response to wind-forcing.

There have been repeated, but inconclusive, attempts to verify the Ekman transport relation directly by using in situ measurement of winds and currents. Although wind-driven transport more or less to the right of the wind is commonly observed, its magnitude has seldom been found to be consistent with Ekman transport computed from estimated wind stress to closer than a factor of about 2 (*6, 7*). This has not been interpreted to mean that Eq. 2 is wrong in principle; there are significant technical difficulties in making accurate in situ current and wind measurements, some of which have only recently been appreciated and overcome (*8*). There are also analysis and interpretation problems in trying to separate the wind-driven current from the measured current (*5*).

In this article we report our efforts to understand the structure of wind-driven currents and transport by analysis and numerical simulation of a set of in situ field measurements. By separating the wind-driven current from the measured current and by constructing a coherent average over a long record, we find that the Ekman transport relation is consistent to within experimental error. The mean current has a spiral structure qualitatively similar to an Ekman spiral. In this case, however, the scale depth depends on the stratification, and in general the dynamics of the spiral appear to be much richer than implied by the original Ekman theory.

LOTUS Field Measurements and Analysis

Our field measurements were acquired from a surface mooring set in the western Sargasso Sea (34°N, 70°W) as part of the Long Term Upper Ocean Study (LOTUS) (*9*). This deployment was termed LOTUS 3, and it spanned 160 days during the summer of 1982. In situ current and temperature measurements were made by Vector Measuring Current Meters (VMCMs) that were designed to measure relatively weak mean currents in the presence of surface gravity wave motion (*8*). These instruments were fixed into the mooring line at depths of 5, 10, 15, 25, 50, 75, and 100 m to provide fairly high vertical resolution of currents in the upper ocean (*10*). LOTUS 3 was the first such long-term deployment of VMCMs.

The surface buoy was a 3-m discus that carried meteorological instruments, including a solar pyranometer. The heat flux at the sea surface was estimated from the measured variables by means of conventional bulk transfer formulas (*11*), and it is thought to be accurate to about 50 W m^{-2} over a long-term average. Wind stress was estimated from measured wind and air-sea temperature differences by using the wind speed and stability-dependent bulk transfer formulas developed by Large and Pond (*12*). Estimated wind stress is thought to be accurate to about 20% over a long-term average. Fair, summer weather typical of the subtropics prevailed during much of this period. Strong solar heating combined with light winds caused the formation of a seasonal thermocline during LOTUS 3 and caused significant diurnal warming of the sea surface on many days (*13, 14*). The upper four VMCMs were crucial for observing the wind-driven current under these conditions, and an even shallower current measurement would have been desirable (*4, 15*).

Given these measurements, the remaining hurdle to overcome before testing Eq. 2 was a poor signal-to-noise ratio. The "signal," the mean wind-driven current, has an amplitude of about 0.05 m sec^{-1}. This is small compared to the pressure-driven current "noise" from tides, inertial motions and nearly geostrophic eddies that together have a root mean square value about five times larger (*9*). An analysis is thus required to separate the wind-driven current from the measured total current.

Because the wind-driven current is likely to be much more strongly surface trapped than the pressure-driven current, the first analysis step is to subtract the current at a deep reference level from the upper ocean current (*7*). The reference depth and lower integration limit for computing transport was taken to be $z_r = 50$ m. This was within the seasonal thermocline for all but the last few weeks of the LOTUS 3 record, and we see no evidence of any important direct wind-driving at that level or deeper.

Our second analysis step is to average the current in a way that is coherent with respect to the wind direction. Wind stress and ocean current are first vector-averaged over each day, then the daily averages are rotated into a coordinate system in which the wind stress is arbitrarily "north," and finally the 160 daily averages are ensemble-averaged to form the mean (*16*). The choice of a daily averaging interval for the first averaging step is not crucial for this purpose, and essentially the same result derives from averaging over portions of 2 days, or one or two inertial periods. In effect, this coordinate system follows the low-frequency variations of wind direction. The resulting mean can be thought of as a sum over all frequencies less than about 0.2 cycle per day and is considerably larger than the usual time average over the full record. For example, the mean wind stress estimated in this way has an amplitude of 0.068 Pa, whereas the simple time average of the vector wind stress has an amplitude of 0.015 Pa. Coherent ensemble averaging thus serves to enhance considerably the signal-to-noise ratio in this data set.

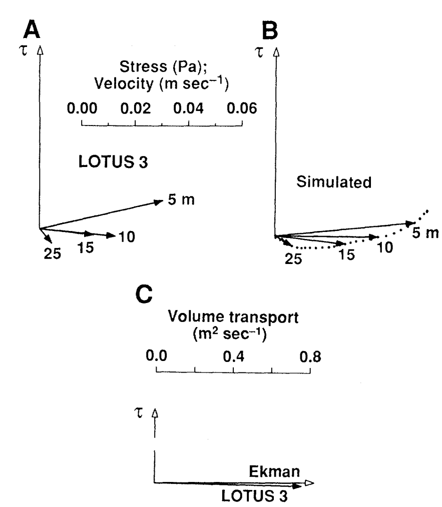

Fig. 1. (**A**) Mean current spiral from the LOTUS 3 data set. The mean has been estimated by an ensemble average over daily averages rotated to a common wind direction (arbitrarily "north" in this and all subsequent figures), and a reference current at a depth of 50 m has been subtracted away. Uncertainties are listed in Table 1. (**B**) Mean current spiral simulated by the numerical model. The vectors correspond to the depths sampled by LOTUS 3, and the dots are at 1-m intervals. The simulated spiral has some shear above a depth of 5 m since on many days the simulated mixed layer was less than 5 m thick during early afternoon. (**C**) Volume transport per unit width computed from the left side of Eq. 1 by using the observed mean currents (solid arrowhead, labeled LOTUS 3) and from the right side of Eq. 1 by using the mean wind stress (open arrowhead, Ekman). Uncertainties are given in Table 1 legend.

Fig. 2. The ensemble-averaged current during the nighttime (2000 to 0800 LST) (left) and during the daytime (0800 to 2000 LST) (right). The upper set of current vectors is from LOTUS 3. The wind stress for the corresponding time of day is plotted as a vector with the mean value shown as a line only. There is very little diurnal variability of wind stress. The lower sets of current vectors (omitting the wind stress vector) are from the numerical model. Numbers at vector tips are the depth in meters.

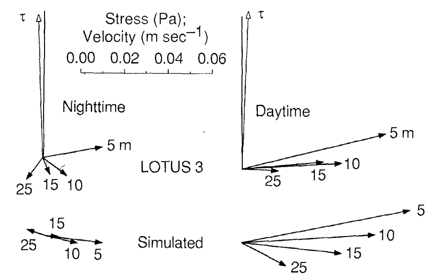

Fig. 3. The diurnal cycle of current at 5 m from the LOTUS 3 data set (**A**) and as simulated (**B**). Numbers at the vector tips are hours (in LST), and the heavy central vector is the mean as in Fig. 1. The 5-m current makes a clockwise rotation during the day, much like an inertial oscillation, and the peak-to-peak amplitude of the diurnal cycle is roughly twice the mean value.

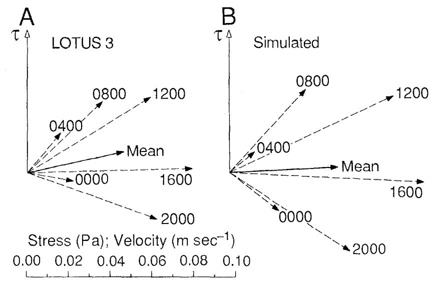

Transport and the Mean Current Spiral

Mean current estimated by the coherent ensemble-averaging procedure described above is shown in Fig. 1A for the four VMCM depths above 50 m; deeper values and standard errors are in Table 1 (*17*). The mean values at 15 m and above are several times larger than their standard error and in this regard are fairly well defined; the mean value at 25 m is comparable to its standard error and not clearly distinguishable from zero. Transport was calculated from the mean current by a trapezoidal rule integration from $z_r = 50$ m to the surface and by assuming linear extrapolation from 5 m to the sea surface by means of the 10- to 5-m gradient. The standard error on the mean transport was computed from daily estimates of transport and is given in Table 1 (*18*).

An important result of this study is that the Ekman transport computed from the mean wind stress (Table 1) is found to be consistent with the observed transport to within about 10% in magnitude and about 5° in direction (Fig. 1C). This is within the statistical uncertainty on the observed transport, about 20%, and the uncertainty on Ekman transport arising from uncertainty of the mean stress, also roughly 20%. It could be argued that the physical basis of the Ekman transport relation is so compelling that the apparent success in verifying the Ekman relation represents not so much a test of a momentum balance, as it does a milestone for upper ocean observation methods.

The scale depth of the mean current and transport depends on turbulent mixing and cannot be presumed to be known the way a momentum balance might be. In this case we find that the wind-driven transport is strongly surface trapped, with roughly 95% of the transport occurring within the upper 25 m of the water column and roughly 60% within the upper 10 m. This strong surface trapping of transport is a surprising result considered further in the next section.

The current vector decays and turns to the right with increasing depth, so that mean current has a spiral-shaped vertical structure somewhat like an Ekman spiral. There are some differences in detail, however. Between 5 and 25 m the e-folding scale of amplitude is only about 12 m. From this scale and from Eq. 1 we can infer an effective viscosity $A = 60 \times 10^{-4}$ m^2 sec^{-1}, which is in the low range of values reported from the upper ocean (*2, 3*). The rate of rightward turning with depth gives a different and inconsistent estimate of A. The current vector at a depth of 5 m is about 80° to the right of the wind, and the further rightward rotation with depth is only about 20° over an e-folding scale, or roughly one-third of the rotation expected in an Ekman spiral [suggested also in (*6*) and (*19*)]. The A inferred from the rotation with depth is about 540×10^{-4} m^2 sec^{-1} or almost an order of magnitude larger than A inferred from the e-folding scale of amplitude. From this it appears that the classical Ekman spiral, and by inference the simple diffusion process of the Ekman model, is not appropriate for the conditions of this data set. We suspect that the main shortcoming of the Ekman and the turbulent Ekman models is that they attempt to model the current profile alone and neglect the often crucial effects of stable density stratification.

Surface Trapping and Stratification

Recent field studies (*6*) have shown that even the rather small stratification that occurs as part of the upper ocean's diurnal cycle (*20, 21*) can be sufficient to greatly reduce the depth over which turbulent mixing distributes the momentum flux supplied by wind stress and can thus lead to a surface-trapped current profile. To test whether stratification may cause the surface trapping of mean current seen here we can attempt to model the current profile from the observed wind stress and thermal stratification (density variations are dominated by temperature variations in this case). Upper ocean temperature profiles commonly show a vertically homogenous surface layer, or mixed layer, of depth h. We assume that temperature and current are mixed in a similar way and that the stratification at the base of the temperature mixed layer marks the depth of vertical turbulent mixing of momentum that is supplied at the surface by wind stress [a more refined view is given in (*6*)]. Thus the mixed layer feels a wind-driven acceleration $\tau/\rho h$, while the acceleration below the mixed layer is zero. The depth of the mixed layer is highly time dependent and is estimated at hourly intervals from VMCM-measured temperatures as the depth over which temperature is uniform to within 0.05°C of the value measured just below the buoy hull at a depth of 0.2 m. The wind-driven acceleration was computed for each VMCM depth over the full record of LOTUS 3 and the mean acceleration was computed by the same coherent ensemble-averaging procedure used on measured current. Finally, the mean current is presumed to be in an Ekman momentum balance, so that the mean acceleration is divided by f to estimate the current amplitude (direction, presumably, is to the right of the wind). At depths of 5, 10, 15, and 25 m, where the observed current amplitude is 0.047, 0.028, 0.020, and 0.004 m sec^{-1}, respectively, the inferred current amplitude is 0.041, 0.027, 0.018, and 0.006 m sec^{-1}, respectively, or very similar. These amplitudes provide further evidence that the mean current is in an Ekman momentum balance and also suggest that it will generally be necessary to understand the variation of upper ocean stratification in order to understand and model the structure of the current profile.

In the LOTUS 3 data set the upper ocean stratification and depth of the mixed layer varied on two important time scales. The seasonal variation in heat flux caused a seasonal cycle in upper ocean stratification that had a surface amplitude, or range, of about 10°C (*14*). On most days the diurnal cycle of solar heating caused a diurnal cycle in the upper ocean stratification that had a surface amplitude of typically 0.3°C, but occasionally exceeded 2°C (*13, 14*). Depth of the mixed layer went through a diurnal cycle having a midday minimum of typically 2 to 10 m, depending on the strength of the wind stress and solar heating, and a nighttime maximum of typically 10 to 30 m, depending on wind stress and heat loss, and often limited by the depth of seasonal stratification. During some weeks in midsummer the seasonal stratification was as shallow as 10 to 15 m and thus contributed significantly to the stratification effect on the current profile. The diurnal cycle also had an important and somewhat disproportionate effect because the depth of the surface mixed layer is determined by the shallowest stratification, even if only a few hundredths of a degree Celsius, which was often part of the diurnal cycle.

The diurnal cycle of current that accompanies the diurnal cycle of stratification can be seen by splitting the daily averages into a nighttime piece [2000 "local solar time" (LST) to 0800 LST], and a daytime piece (0800 LST to 2000 LST), and then ensemble-averaging each separately as before by using the daily average wind stress to define "north" (Fig. 2). The sum of the nighttime and daytime pieces gives the mean of Fig. 1. In a similar way, the 5-m current is shown in Fig. 3 at 4-hour intervals through the (ensemble-averaged) day.

During midday when the mixed layer is shallowest, the current at a depth of 5 m accelerates downwind and simultaneously is turned to the right by the Coriolis force. At this latitude the diurnal frequency and inertial frequency f are nearly equal, and hence the diurnal cycle of current has the character of an inertial oscillation. The 5-m current reaches a maximum of about 0.09 m sec^{-1} at around 1600 LST, just as it turns 90° to the right of the wind stress. Heat loss and wind stress during the night often erase much of the diurnal stratification and shear, and the 5-m current reaches a minimum of about 0.01 m sec^{-1} at around 0400 LST. Figures 2 and 3 show that much of the surface trapping of the mean current spiral comes from the daytime half of the diurnal cycle.

Numerical Simulations and Experiments

A consistent picture of the diurnal variability and the mean current spiral emerges from simulations made with a numerical model of the ocean surface mixed layer (*6*). For this model and other models of the mixed layer, it is assumed that temperature and current are mixed in a similar way and that wind stress is absorbed by the mixed layer exactly as described above. The issue for these models is then to calculate the depth of the mixed layer (*22*). In this model, the depth is determined by a stability condition on a Richardson number that depends on the current shear and stratification at the base of the mixed layer. When current shear becomes large enough compared to the stratification to violate the stability condition, the mixed layer is presumed to deepen by turbulent mixing in order to relieve the instability.

Integration was carried out as in (*13*) by using the 160-day record of estimated wind stress and surface heat fluxes; the simulated current was then analyzed as described for the LOTUS 3 data although with no need to subtract a reference current. Model simulations of transport always satisfy the Ekman transport relation since only wind stress and Coriolis forces act on the water column. The more interesting model results are the overall shape and scale depth of the mean current spiral (Fig. 1B), the night-to-day variation of current (Fig. 2), and the diurnal cycle of 5-m current (Fig. 3B).

The simulated 5-m current has an amplitude and phase over the diurnal cycle very similar to the one observed, suggesting that the model gives a reasonably good account of the hour-by-hour effect of wind stress and solar heating on the depth of the surface mixed layer and on the vertical structure of the wind-driven current. Not surprisingly then, the simulated mean current spiral is also fairly similar to the observed mean spiral, e-folding over a depth of about 12 m (Fig. 1B). We know of nothing that makes this result unique to this specific model and expect that other upper ocean models (*20, 21, 23, 24*) would perform as well as this one if driven with the same wind stress and the same diurnally varying heat flux (*25*).

A series of numerical experiments have been run to see how the simulated mean current spiral depends on external parameters when the stable stratification is produced by the diurnal cycle (no seasonal variations). A standard case is defined to have a heat flux made up of solar insolation with a magnitude of 650 W m^{-2}, a half-period of 12 hours, and a steady heat loss of 150 W m^{-2}, so that the net surface heat flux Q = 500 W m^{-2} at the daily maximum. Wind stress is assumed steady with magnitude τ = 0.1 Pa, and the Coriolis parameter $f = 6.15 \times 10^{-5}$ sec^{-1} (corresponding to 25°N). The standard values of Q, τ, and f were each multiplied in turn by factors of 0.5 and 2. Figure 4 shows the resulting mean current spirals from each of the seven experiments. The central spiral is the standard case.

In all cases the Ekman transport relation is satisfied exactly, and some of the variations of the spiral follow directly from the τ/f

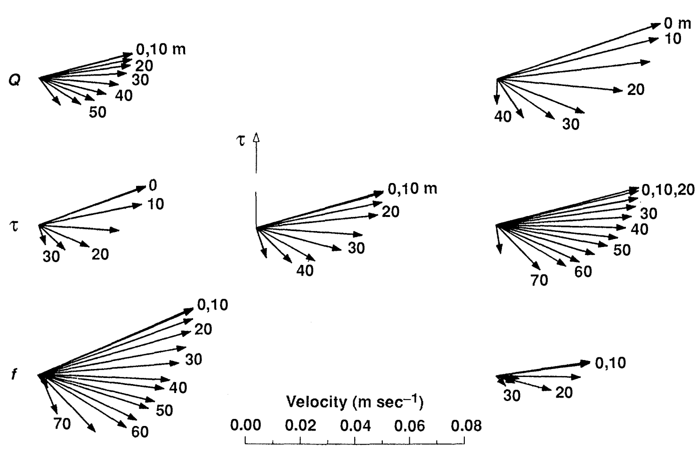

Fig. 4. Mean current spirals produced by numerical experiments. The standard case (central spiral) has Q = 500 W m^{-2}, τ = 0.1 Pa, and f corresponding to 25°N. Each of Q, τ, and f have been multiplied by a factor of 0.5 (left column) or 2 (right column). For example, the upper left spiral has Q = 250 W m^{-2}, and τ and f the same as the standard case. Numbers at the tips of the vectors are the depth in meters.

Table 1. Statistics on the mean current and transport are given for components in the crosswind direction (positive to the right of the wind) and the downwind direction. Uncertainties on the in situ data are statistical standard errors (*16, 17*); 90% confidence limits are larger by a factor of 1.7, and 95% confidence limits are larger by a factor of 2.0. The transport values (in square meters per second) were as follows: The observed crosswind transport was 0.76 ± 0.19; the downwind transport, −0.02 ± 0.14. The Ekman crosswind transport was 0.82 ± 20%; downwind transport, 0. The Ekman transport was computed by using the estimated mean stress magnitude 0.068 Pa, which is presumed to be uncertain to 20% because of uncertainty inherent in the bulk aerodynamic method.

Depth (m)	Crosswind current (m sec^{-1})	Downwind current (m sec^{-1})
5	0.046 ± 0.012	0.010 ± 0.007
10	0.028 ± 0.007	−0.003 ± 0.004
15	0.020 ± 0.007	−0.002 ± 0.005
25	0.004 ± 0.004	−0.005 ± 0.004
50*		
75	0.006 ± 0.003	−0.002 ± 0.004
100	0.011 ± 0.006	−0.007 ± 0.006

*The 50-m depth was chosen as the reference level, where the simple time-mean velocity was 0.181 m sec^{-1} westward and 0.007 m sec^{-1} northward.

dependence of Ekman transport (Eq. 2). For example, either doubling τ (middle row, right column, Fig. 4) or halving f (lower row, left column, Fig. 4) causes the Ekman transport to double and produces a similar change in the spiral (the angle between the wind and surface current decreases slightly with decreasing f). Looking from left to right across the middle row, one sees that although the transport increases by a factor of 4 along with τ, there is very little increase in the amplitude of the surface current, $\mathbf{V}_s$. The increase in transport is taken up primarily by an increase in the e-folding scale of the spiral, rather than by an increase in the current amplitude. From Fig. 4 (middle row) it appears that the e-folding scale is proportional to τ and that $\mathbf{V}_s$ is nearly independent of τ. When Q is increased (left to right across the top row, Fig. 4), the spiral is more strongly surface trapped and $\mathbf{V}_s$ increases roughly as $Q^{1/2}$ even though the transport is unchanged. This tendency for $\mathbf{V}_s$ to increase with Q while being nearly independent of τ is a property of the Richardson number closure of this model described in (*6*).

Discussion

The principal results of this analysis are that (i) the Ekman transport relation was found to give an estimate of wind-driven transport consistent with the transport estimated from in situ current measurements, and (ii) mean current was found to have a spiral-like structure that is strongly surface trapped on account of solar heating and the resulting stable stratification. A simple numerical model that takes account of the important effect of stratification was successful in simulating the diurnal variability of current and the mean current spiral.

We suggest that the current profiles described here be termed "stratified" Ekman spirals, both to credit Ekman for the insight he gave to the problem of wind-driven ocean currents and to emphasize that the mean current spiral in the upper ocean is very closely linked to the stratification. Numerical experiments have given some indication of how the spiral might vary when solar heating during the diurnal cycle controls the stratification. But there are common circumstances in which solar heating will not be controlling, for example, during mid-latitude winter when sustained cooling of the ocean can produce very deep mixed layers. The classical or turbulent Ekman models may be more appropriate for those conditions, but the observations that might tell this have not been made. Modern measurement systems like the LOTUS surface buoy and VMCM instruments are able to provide the observational basis needed to build and test models for these and other regimes of the upper ocean.

REFERENCES AND NOTES

1. V. W. Ekman, *Ark. Mat. Astron. Fys.* **2**, 52 (1905).
2. G. L. Pickard and S. Pond, *Introductory Dynamical Oceanography* (Pergamon, Elmsford, NY, ed. 2, 1983).
3. M. W. Stacey, S. Pond, P. H. LeBlond, *Science* **233**, 470 (1986).
4. N. E. Huang, *J. Fluid Mech.* **91**, 191 (1979).
5. A. Gill, *Atmosphere-Ocean Dynamics* (Academic Press, New York, 1982).
6. J. F. Price, R. A. Weller, R. Pinkel, *J. Geophys. Res.* **91(C7)**, 8411 (1986).
7. R. E. Davis, R. DeSzoeke, D. Halpern, P. Niiler, *Deep Sea Res.* **28**, 1427 (1981).
8. R. A. Weller and R. E. Davis, *ibid.* **27**, 565 (1980).
9. M. G. Briscoe and R. A. Weller, *Dyn. Atmos. Oceans* **8**, 243 (1984).
10. S. A. Tarbell, N. J. Pennington, M. G. Briscoe, *Woods Hole Oceanogr. Inst. Tech. Rep. WHOI-84-36* (1984).
11. C. Deser, R. A. Weller, M. G. Briscoe, *Woods Hole Oceanogr. Inst. Tech. Rep. WHOI-83-32* (1983).
12. W. G. Large and S. Pond, *J. Phys. Oceanogr.* **11**, 324 (1981).
13. L. Stramma, P. Cornillon, R. A. Weller, J. F. Price, M. G. Briscoe, *ibid.* **16**, 827 (1986).
14. C. M. Bowers, J. F. Price, R. A. Weller, M. G. Briscoe, *Woods Hole Oceanogr. Inst. Tech. Rep. WHOI-86-5* (1986).
15. J. G. Richman, R. A. DeSzoeke, R. E. Davis, *J. Geophys. Res.* **92(C3)**, 2851 (1987).
16. The VMCM at a depth of 5 m failed abruptly after about 86 days. We did not truncate the other records to this length after determining that (i) the mean wind stress and heat fluxes over the first 86 days were almost identical to the means over the full 160 days and (ii) numerical simulations gave nearly identical results over these two periods.
17. The number of effective degrees of freedom used to estimate standard error was taken to be twice the integral time scale, 1.5 days, divided into the record length in days. The integral time scale was surprisingly short because most variability in current is contributed by tides and inertial motions rather than by more slowly varying geostrophic eddies.
18. A different and possibly more troublesome error in estimating transport might result from the choice of the reference depth, z_r = 50 m. A shallower reference depth, 25 m, gives almost the same result for transport, as there is very little vertical shear of mean current from 25 to 50 m. However, the next deeper, possible reference depth, 75 m, gives a considerably smaller transport, only about 0.4 m^2 sec^{-1}, although the current spiral is little altered. Still deeper reference depths cause even greater change in estimated transport since the current amplitude relative to 50 m increases with increasing depth. This is inconsistent with the notion of wind-forcing at the surface. On the basis of the overall structure of the mean current, and to a lesser degree the numerical simulations, z_r = 50 m is appropriate for LOTUS 3. In future experiments it would be desirable to observe the mass field with sufficient precision to estimate the vertical structure of the horizontal pressure gradient. This would presumably allow the reference depth to be taken deeper in the water column without incurring excessive contamination from vertically sheared, pressure-driven currents. It would also be beneficial to measure the sea-surface pressure, and thereby estimate the absolute, pressure-driven current.
19. R. A. Weller, *J. Geophys. Res.* **86**, 1969 (1981).
20. J. Kondo, Y. Sasano, T. Ishii, *J. Phys. Oceanogr.* **9**, 360 (1979).
21. J. D. Woods and V. Strass, *Q. J. R. Meteorol. Soc.* **112**, 29 (1986).
22. The Ekman model and mixed-layer models take the opposite extremes regarding the depth distribution of turbulent mixing. The Ekman model presumes constant turbulent mixing intensity represented by a finite A, whereas mixed-layer models presume infinite vertical mixing down to a depth h and vanishing mixing below. These both must be idealizations. A wide range of modern field observations (*6, 7*) favors the mixed-layer model for descriptions of the instantaneous current or temperature profiles. In cases where h varies over a wide range as it does here, the mean current and temperature profiles produced by a mixed-layer model will tend to have a smooth distribution (*7*) much as would be expected from an Ekman-like diffusion process. The major advantage of mixed-layer models, even if only the mean profile were of interest, is that they readily include stratification.
23. G. L. Mellor and P. A. Durbin, *J. Phys. Oceanogr.* **5**, 718 (1975).
24. R. E. Davis, R. DeSzoeke, P. Niiler, *Deep Sea Res.* **28**, 1453 (1981).
25. Model experiments provide a means to make a consistency check on the assumption made implicitly here that the ensemble average could be interpreted as if the wind stress had held constant at the mean value of 0.068 Pa over the entire record. This is found to be approximately correct. Even more, the model gives almost the same result when driven with the observed mean wind stress and the observed ensemble-averaged daily surface heating, which had a noontime maximum insolation of 730 W m^{-2} with a half-period of 11 hours and a constant heat loss of 100 W m^{-2}. This simple prescription for LOTUS 3–forcing could be applied to other upper ocean models for comparison with the results here.

26. We thank the Office of Naval Research for their support of the LOTUS project through contract N00014-76-C-0197, NR 083-400, and for support of J.F.P., R.A.W., and R.R.S. through contract N00014-84-C-0134, NR 083-400 with the Woods Hole Oceanographic Institution. The LOTUS project was begun by M. Briscoe who planned and supervised much of the fieldwork, assisted by R. Trask and members of the Woods Hole Buoy Group; their efforts made these measurements possible. We thank P. Flament, V. Kaharl, A. Plueddemann, J. McWilliams, K. Brink, and P. Richardson for comments on the manuscript, and N. Pennington and C. Light for assistance with data processing and analysis. This is contribution 6520 of the Woods Hole Oceanographic Institution.